Unizik Journal of Technology, Production and Mechanical Systems (UJTPMS)

journal homepage: https://journals.unizik.edu.ng/index.php/ujtpms/about
PRINT ISSN: 1115-7143 || ONLINE ISSN: 1115-7453

Effects of Ambient Conditions on the Performance of Gas Turbine: A Parametric Analysis

Chukwuneke Jeremiah Lekwuwa[1*], Okechi Lubee Emeana[1], Amaefule Desmond Okechukwu[2], Unegbu Chukwudi Ignatius[3], Ekechi Augustine Tochukwu[4], Egbuna Ikechukwu.Chukwuka[1], Osazuwa Orobosa Kingsley[1].

[1]Department of Mechanical Engineering, Nnamdi Azikiwe University, Awka, NIGERIA
[2]Department of Agricultural & Bioresource Engineering, Nnamdi Azikiwe University, Awka, NIGERIA
[3]Shell Nigeria Exploration and Production Company, Lagos, NIGERIA
[4]Department of Chemical Engineering, Nnamdi Azizikwe University, Awka, NIGERIA

ARTICLE INFO

Article history:
Received March 25, 2025
Revised April 12, 2025
Accepted April 13, 2025

Available online April 21, 2025

Keywords:
Power plant, Gas turbine, Efficiency, Simulation, Ambient temperature, Relative humidity, Parametric analysis, Energy, Thermodynamics

ABSTRACT

Gas turbine performance is greatly dependent on ambient environmental conditions, specifically pressure, temperature, and relative humidity. In this paper, the performance of a gas turbine power plant is studied using a parametric analysis. Thermodynamic relationships were used to develop mathematical models that simulated the performance of the gas turbine under varying operating conditions; ambient temperature (AT) and relative humidity (RH). The gas turbine used in the simulation is located at the Ughelli Transcorp power plant in Nigeria. The simulation was carried out using Runge-Kutta method, and the model shows that operational parameters like AT and RH significantly impact a gas turbine power plant's performance. The findings indicate that increasing the RH from 40% to 50% reduces cycle efficiency by 0.022 % while increasing power output. A 25% increase in RH results in a 55% increase in compression power consumption. Furthermore, the power output and thermal efficiency increase as the AT and RH increase. The findings indicate that both AT and RH have a significant impact on the overall performance of the gas turbine plant. As a result, the thermodynamic parameters are economically feasible in terms of cycle performance and advantageous for gas turbine operations.

1. Introduction

Electricity is the most rapidly growing form of end-use energy, with an exponential increase in production to meet the ever-growing demand. The rising demand for power in Nigeria has necessitated the construction of power plants capable of producing maximum power output at AT. Electricity in bulk production qualities can be met using gas turbine plants [1]. All over the world, gas turbines are frequently utilized to generate electricity [2]. In hot and dry conditions, gas turbine engine power output is significantly decreased because high input air AT reduces gas turbine air mass flow [3-5]. For example, Nigeria's climate and weather are inconsistent, indicating that the climates in the north and south differ. Therefore, the pre-cooling methods used in southern Nigeria may be inappropriate for the region in the north [6-7]. These gas turbine plants run on fossil fuels, notably natural gas, whose availability is finite. Under static conditions of increase in demand and production, these fossil fuel sources will be exhausted in no distance time [8-10]. Another source of worry is the continued rise in the cost of natural gas as a result of an increase in demand, which generally increases the operation cost per kWh of energy generated [11-13]. Many industries, including refineries and petrochemical factories, employ gas turbines to operate aircraft, generate power and run other machinery [14-16].

The primary goal of turbine inlet air pre-cooling is to boost the gas turbine's net power production when the AT is higher than optimal. The rated capabilities of gas turbines are typically based on the typical AT of 15 ºC and 14.7 psi at sea level, according to Al-Tori [17]. According to Mahapatra & Sanjay [18], the times when the electricity demand is highest are typically when gas turbines suffer the biggest output power losses. When the intake temperature is between 15 and 25 ºC, about 7% of a gas turbine's nominal power can be lost, and when the AT is above 25 ºC, the loss may be as high as 15% [19-21]. Plant performance will be

**Corresponding author:* jl.chukwuneke@unizik.edu.ng

improved during high AT by lowering the temperature of the air entering the compressor below the ambient [22-23]. A turbine's output is significantly impacted by the AT, with power output falling by 0.54 to 0.9°C for every 1°C rise in temperature. Gas turbines may experience power output declines between 14% and 20% when AT rises from about 15 to 35°C [24]. Temperature has a significant impact; for every 56°C rise in temperature, output work grows by about 10%, and efficiency rises by around 1.5% [25].

Ensuring gas turbines run at maximum efficiency is a key primary goal for any operation. In the current economic climate, anything that increases productivity and enhances profit is welcome, as most of the operating cost of a gas turbine plant is the cost of the fuel used to power the turbine plant. Also tied to improvement in efficiency is the net output power of the gas turbine plant, a high value of load factor is desired for the economic operation of the plant and to produce electricity at less cost [26-27]. The climate has a significant impact on how well a gas turbine performs [25]. The AT has a substantial impact on a gas turbine's performance, specifically its output and energy efficiency [1,21]. Any rise in AT and RH decreases the ambient air density [11]. The load factor is directly linked to kWh produced by the gas turbine plant. This paper seeks to focus on the impact of AT on the performance of the gas turbine plant as regards the specific power output, compressor power, combustion heat supplied, exhaust energy, and efficiency of the gas turbine plant. Thus the objectives of this study are to: demonstrate analytically that more power can be produced from a gas turbine plant by suitable conditioning of the ambient air at the compressor inlet; thermodynamically model the performance of the gas turbine and evaluate the ambient temperature and relative humidity; identify the optimal design parameters and determine the impact of the deviations of these parameters; and determine the performance of a gas turbine power plant utilizing the effect of operating conditions.

2. Thermodynamic Model for Parametric Analysis of Gas Turbine Plant

2.1 Thermal Analysis of Gas Turbine Plant

The parametric study relies on the operating conditions of the Ughelli Transcorp Power Plant, as shown in Fig. 1. Table 1 displays the plant specifications.

Table 1 – Specifications of the plant

Turbine alternator power output	**25 MW**
Alternator Current	1100 A
Alternator output voltage	11 KV
Alternator frequency	50 Hz
Efficiency of the gas turbine	0.34
Alternator speed	7280 rpm
Turbine inlet temperature	1200 ºC
Exhaust gas temperature	520 ºC
Gas turbine inlets pressure	1.4 MPa
Turbine type	3
Compressor stages	17
Cooling oil inlet temperature	59 ºC

Fig. 1 – Ughelli transcorp power plant

Based on the thermodynamic characteristics of humid air, the amount of moisture in the air can be calculated as [28];

$$\omega = \frac{m_w}{m_a} \tag{1}$$

The abbreviations m_w, m_a and ω stand for the mass of water vapour, dry air, and specific humidity, respectively.

Since both masses occupy the same volume then;

$$\omega = \frac{m_w/V}{m_a/V} = \frac{1/v_w}{1/v_a} = \frac{v_a}{v_w} \tag{2}$$

Where v_a, v_w is the specific volume of dry air and the specific volume of water vapour in m^3/kg, respectively.

Both the vapour and dry air are considered perfect gas, hence;

$$m_w = \frac{P_w V}{R_w T} \quad \text{and} \quad m_a = \frac{P_a V}{R_a T} \tag{3}$$

$$R_a = \frac{R_o}{M_a} \quad \text{and} \quad R_w = \frac{R_o}{M_w} \tag{4}$$

Where R_o is the universal gas constant, M_a and M_w are the molar mass of dry air and water vapor, respectively, R_a is the characteristic air gas constant, and R_w is a characteristic water vapor gas constant.

Substituting Eq. (4) into Eq. (3);

$$m_w = \frac{P_w V M_w}{R_o T} \quad \text{and} \quad m_a = \frac{P_a V M_a}{R_o T} \tag{5}$$

Substituting Eq. (5) into Eq. (1);

$$\omega = \frac{M_w}{M_a} \times \frac{P_w}{P_a} \tag{6}$$

Where $M_w = 18\ kg/kmol$, and $M_a = 28.96\ kg/kmol$

Substituting the values into Eq. (6);

$$\omega = 0.622 \frac{P_w}{P_a} \tag{7}$$

According to Gibbs-Dalton law, the total pressure, P, of the atmosphere is obtained as:

$$P = P_w + P_a \tag{8}$$

Where P_w *and* P_a are partial pressure of water vapour and dry air, respectively and P is barometric pressure in N/m^2.

Substituting Eq. (8) into Eq. (7), thus;

$$\omega = 0.622 \frac{P_w}{P - P_w} \tag{9}$$

According to Ibrahim and Rahman [28], the RH is defined mathematically as;

$$\phi = \frac{m_w}{m_{w,s}} \tag{10}$$

Hence; $$m_{w,s} = \frac{P_s V}{R_w T} \tag{11}$$

Where P_s is the saturation pressure of the mixture at its temperature.

Substituting Eqs. (3) and (11) into Eq. (10) yields;

$$\phi = \frac{P_w}{P_s} \tag{12}$$

Substituting Eq. (12) into Eq. (9) yields:

$$\omega = \frac{0.622 \phi P_s}{P - \phi P_s} \tag{13}$$

The enthalpies of dry air and water vapour are summed to determine the total enthalpy of atmospheric air, which is expressed as [29]:

$$h = h_a + \omega h_w \tag{14}$$

h_a *and* h_w stand for the enthalpy of dry air and water vapour, respectively.

The enthalpy of water vapour can be obtained from tables or determined approximately as;

$$h_w = 2500.9 + 1.82T \tag{15}$$

Where T is the temperature of the water vapour.

2.2 Thermodynamic Modelling of Gas Turbine Plant

The single gas turbine is revealed schematically in Fig. 2(a). Fresh air from the atmosphere is continuously brought into the circuit, and energy is added by the working fluid itself as the fuel in it burns. The turbine, which generates work and eventually releases the by-products of combustion into the atmosphere, expands the combustion products. The temperature-entropy diagram in Fig. 2(b) shows the ideal and actual processes as full and dotted lines, respectively. The thermodynamics cycle on which this gas turbine operates is the Brayton (Joule) cycle, which can be analyzed using Fig. 2(b).

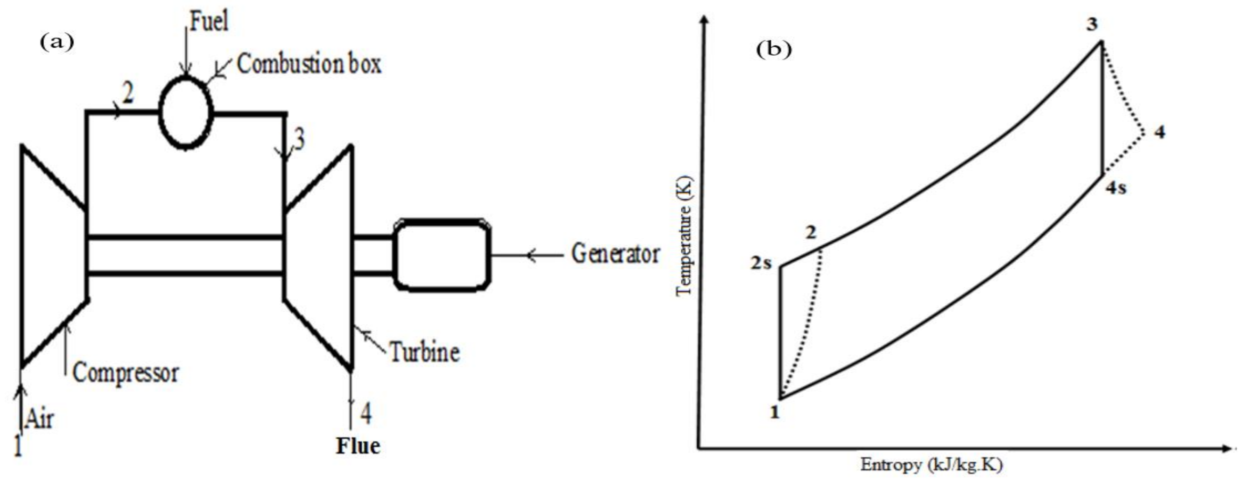

Fig. 2 - (a) Gas turbine unit (b) gas turbine temperature-entropy diagram

Using the first law of thermodynamics to describe an open thermal system [25];

$$\dot{Q} - \dot{W}_{shaft} = \sum_m \dot{m}\left(h + \frac{v^2}{2} + gz\right)_{in} - \sum_m \dot{m}\left(h + \frac{v^2}{2} + gz\right)_{out} \quad (16)$$

The gravitational potential energy (gz) and kinetic energy ($v^2/2$) are not major elements for this analysis and can be neglected. For every control volume in steady-state with minimal kinetic and potential energy changes, the energy balance for the first law changes;

$$\dot{Q} - \dot{W}_{shaft} = \dot{m}(h_{out} - h_{in}) \quad (17)$$

The energy balance equations for various parts of the gas turbine plant in Fig. 2 are as follows;

2.2.1 Compressor Power Model

The compressor compression ratio (r_p) can be expressed as;

$$r_p = \frac{P_2}{P_1} \quad (18)$$

Where P_1 and P_2 are, respectively, the compressor's inlet and exit air pressures.

Using the concept of isentropic efficiency and neglecting velocity across the inlet and exit of the compressor, regarding the gas turbine T-S diagram. The compressor isentropic efficiency, which ranges from 85% to 90%, is stated as;

$$\eta_c = \frac{T_{2'} - T_1}{T_2 - T_1} \quad (19)$$

η_c stands for the compression isentropic efficiency, T_1 and T_2 are, respectively, the compressor inlet and exit air temperatures, and $T_{2'}$ is the compressor isentropic outlet temperature.

For compression process 1–2;

$$T_2 = T_1\left(\frac{P_2}{P_1}\right)^{\frac{\gamma_a - 1}{\gamma_a}} = T_1(r_p)^{\frac{\gamma_a - 1}{\gamma_a}} \quad (20)$$

Where $\gamma_a(\text{specific heat capacity of air}) = 1.4$.

For a given pressure ratio;

$$T_2 - T_1 = \frac{1}{\eta_c}(T_{2'} - T_1) = \frac{T_1}{\eta_c}\left(\frac{T_{2'}}{T_1} - 1\right) \quad (21)$$

The pressure ratio and inlet compressor temperature can be used to calculate the compressed air temperature as follows;

$$T_2 = T_1\left[1 + \frac{(r_p)^{\frac{\gamma_a - 1}{\gamma_a}} - 1}{\eta_c}\right] \quad (22)$$

Where T_1 is the ambient temperature, T_2 is the actual compressor outlet temperature of the compressed air entering the combustion chamber.

The power consumed by the compressor can be expressed as;

$$\dot{W_c} = \dot{m}_a C_{pa}(T_2 - T_1) \quad (23)$$

At full load, the work rate of the compressor, W_c can be expressed using the pressure ratio and the inlet compressor temperature as:

$$\dot{W}_c = \frac{\dot{m}_a C_{pa} \times T_1 \left[(r_p)^{\frac{\gamma_a - 1}{\gamma_a}} - 1 \right]}{\eta_c} \quad (24)$$

Eq. (24) can be used to fit temperatures between 200 K and 800 K, where C_{pa} is the specific heat of air, which is thought to be a function of temperature [28];

$$C_{pa}(T) = 1.0189 \times 10^3 - 0.13784T_a + 1.9843 \times 10^{-4}T_a^2 + 4.2399 \times 10^{-7}T_a^3 - 3.7632 \times 10^{-10}T_a^4 \quad (25)$$

Where $T_a = \frac{T_2 - T_1}{2}$.

Thus, in terms of the specific humidity and AT, the actual power consumed by the compressor can be estimated as;

$$\dot{W}_c = \dot{m}_a(1 + \omega)[C_{pa}(T_2 - T_1) + \omega(h_2 - h_1)] \quad (26)$$

By substituting Eq. (22) into Eq. (26) as follows, in terms of the pressure ratio and the inlet compressor temperature, Eq. (26) can be stated.;

$$\dot{W}_c = \dot{m}_a(1 + \omega)[\frac{C_{pa}T_1}{\eta_c}\left((r_p)^{\frac{\gamma_a - 1}{\gamma_a}} - 1 \right) + \omega(h_2 - h_1)] \quad (27)$$

2.2.2 Combustion Chamber Model

The compressed air is fed into the combustion chamber, where a quantity of fuel is introduced and ignited to release a large quantum of energy, resulting in a high-temperature gaseous mixture. The stoichiometric ratio is approximately 15:1, but the actual fuel ratio is in the 100:1 range [30]. The mass of fuel needed to reach a specific combustion chamber exit temperature is determined by the mass and energy balance applied over the control volume of the combustion chamber.

Mass and energy balance gives;

$$\dot{m}_g = \dot{m}_a + \dot{m}_f \quad (28)$$

Therefore; $\left(\dot{m}_a C_{pa} T_2\right) + \left[\left(\dot{m}_f \times LHV\right) + \left(\dot{m}_f C_{pf} T_f\right)\right] = (\dot{m}_a + \dot{m}_f) C_{pg} T_i$ (29)

Rearranging Eq. (29) yield;

$$\left(\dot{m}_a C_{pa} T_2\right) + \dot{m}_f (LHV + C_{pf} T_f) = (\dot{m}_a + \dot{m}_f) C_{pg} T_i \quad (30)$$

Where $\dot{m}_f, \dot{m}_a$ are respectively, mass flow rate of fuel and air, LHV is a low heating value, $T_i = T_3, T_f$ are respectively, turbine inlet temperature and temperature of the fuel, C_{pf}, C_{pg} are respectively, the specific heat of fuel and combustion product; Eq. (31) can be used to fit the specific heat capacity of the combustion product, which is thought to be a temperature-dependent function, for temperatures between 1000K and 1500K. [31];

$$C_{pg}(T) = 1.8083 - 2.3127 \times 10^{-3}T + 4.045 \times 10^{-6}T^2 - 1.7363 \times 10^{-9}T^3 \quad (31)$$

From Eq. (31), the fuel-air ratio (f) is expressed as;

$$f = \frac{\dot{m}_f}{\dot{m}_a} = \frac{(C_{pg} \times T_i) - (C_{pa} \times T_2)}{LHV - (C_{pg} \times T_i)} \quad (32)$$

The heat transfer or heat supplied due to combustion in the combustion chamber by application of the steady flow energy equation is given as;

$$\dot{Q}_s = \dot{m}_g C_{pg}(T_i - T_2) \quad (33)$$

Rearranging Eq. (33) and expressed in terms of the pressure ratio and the inlet compressor temperature, the specific value of the heat transfer is given as;

$$Q_s = C_{pg}[T_i - T_1\left(1 + \frac{(r_p)^{\frac{\gamma_a - 1}{\gamma_a}} - 1}{\eta_c}\right) \quad (34)$$

Thus, in terms of the specific humidity, application of the first law of thermodynamics in the combustor yields the energy balance;

$$\dot{Q}_s = \left[\dot{m}_a(1 + \omega) + \dot{m}_f\right]\left[C_{pg}(T_i - T_2) + \omega(h_2 - h_1)\right] \quad (35)$$

Since, $\dot{Q}_s = \dot{m}_f LHV$;

Therefore; $\dot{m}_f LHV = \left[\dot{m}_a(1 + \omega) + \dot{m}_f\right]\left[C_{pg}(T_i - T_2) + \omega(h_2 - h_1)\right]$ (36)

Where h_3 is the enthalpy of water vapour at the turbine inlet, h_2 is the enthalpy of water vapour at the compressor outlet.

2.2.3 Gas Turbine Model

Eq. (37) can be used to calculate the gas turbine efficiency [30];

$$\eta_T = \frac{\dot{W}_n}{\dot{Q}_s} \tag{37}$$

Eq. (38) is used to compute the gas turbine net work as;

$$\dot{W}_n = \dot{W}_T - \dot{W}_c \tag{38}$$

Therefore; $\eta_T = \frac{\dot{W}_n}{\dot{m}_f LHV}$ (39)

By application of the steady flow energy equation, the ideal work transfer is given as;

$$\dot{W}_T = \dot{m}_g C_{pg}(T_3 - T_4) \tag{40}$$

Where η_T is the gas turbine efficiency, W_n is a network of the gas turbine, and W_T is shaft work of the turbine.

The isentropic efficiency of the turbine can be written as;

$$\eta_T = \frac{Actual\ work}{Isentropic\ work} = \frac{T_3 - T_4}{T_3 - T_{4'}} \tag{41}$$

Therefore, $T_{4'}$ can be defined as;

$$T_{4'} = \frac{T_3}{(r_T)^{\frac{1-\gamma_g}{\gamma_g}}} \tag{42}$$

Consequently, the turbine pressure ratio, turbine inlet temperature, and turbine exit temperature may be used to express the turbine isentropic efficiency as follows:

$$\eta_T = \frac{1-\left(\frac{T_4}{T_3}\right)}{1-(r_T)^{\frac{1-\gamma_g}{\gamma_g}}} \tag{43}$$

Where r_T is the turbine pressure ratio$= P_3/P_4$, and γ_g is the specific heat capacity of the products of combustion.

From Eq. (43), the actual turbine outlet temperature from the gas turbine is given as;

$$T_4 = T_3\left[1 - \eta_T\left(1 - (r_T)^{\frac{1-\gamma_g}{\gamma_g}}\right)\right] \tag{44}$$

Eq. (44) is substituted into Eq. (40), and the turbine shaft work rate is expressed as a function of the turbine's inlet temperature and pressure ratio;

$$\dot{W}_T = \dot{m}_g C_{pg} T_3 \eta_T \left(1 - (r_T)^{\frac{1-\gamma_g}{\gamma_g}}\right) \tag{45}$$

Eq. (45) minus Eq. (24) provides the gas turbine's network rate in relation to the pressure ratio, compressor input temperature, and turbine inlet temperature;

$$\dot{W}_n = \dot{m}_g C_{pg} T_i \eta_T \left(1 - (r_T)^{\frac{1-\gamma_g}{\gamma_g}}\right) - \frac{\dot{m}_a C_{pa} T_1\left[(r_p)^{\frac{\gamma_a-1}{\gamma_a}} - 1\right]}{\eta_c} \tag{46}$$

The pressure ratio, compressor intake temperature, and turbine inlet temperature are used to express the turbine power output (P) as;

$$P = m_g\left[C_{pg} T_i \eta_T \left(1 - (r_T)^{\frac{1-\gamma_g}{\gamma_g}}\right) - \frac{C_{pa} T_1\left[(r_p)^{\frac{\gamma_a-1}{\gamma_a}} - 1\right]}{\eta_c}\right] \tag{47}$$

Also, using the isentropic relation between state '3' and state '4', substituting Eq. (42) into Eq. (41) gives;

$$T_i - T_4 = \eta_T T_i \left(1 - (r_T)^{\frac{\gamma_g-1}{\gamma_g}}\right) \tag{48}$$

Considering the effect of ambient conditions, the power developed by the turbine can then be evaluated using Eq. (49);

$$W_T = \left[m_a(1+\omega) + m_f\right]\left[C_{pg}(T_i - T_4) + \omega(h_3 - h_4)\right] \tag{49}$$

Where h_4 is the enthalpy of water vapour at the turbine outlet.

Substituting Eq. (48) into Eq. (49), the total power developed in terms of inlet temperature and specific humidity is given by;

$$W_T = \left[m_a(1+\omega)+m_f\right]\left[C_{pg}\left(\eta_T T_i\left(1-(r_T)^{\frac{\gamma_g-1}{\gamma_g}}\right)\right)+\omega(h_3-h_4)\right] \quad (50)$$

The net power developed by the gas turbine in terms of inlet temperature and specific humidity is given as Eq. (51);

$$P = \left[\left(m_a(1+\omega)+m_f\right)C_{pg}(T_i-T_4)+\omega(h_3-h_4)\right]-\left[\left(m_a(1+\omega)C_{pa}(T_2-T_1)\right)+\omega(h_2-h_1)\right] \quad (51)$$

The specific fuel consumption (SFC) is determined by Eq. (52);

$$SFC = \frac{3600\times f}{W_n} \quad (52)$$

$$WR = \frac{\dot{W}_n}{\dot{W}_T} \quad (53)$$

Therefore, the energy of the exhaust gases wasted in the atmosphere can be expressed as:

$$G = \left[m_a(1+\omega)+m_f\right]\left[C_{pg}(T_4-T_1)-\omega(h_4-h_1)\right] \quad (54)$$

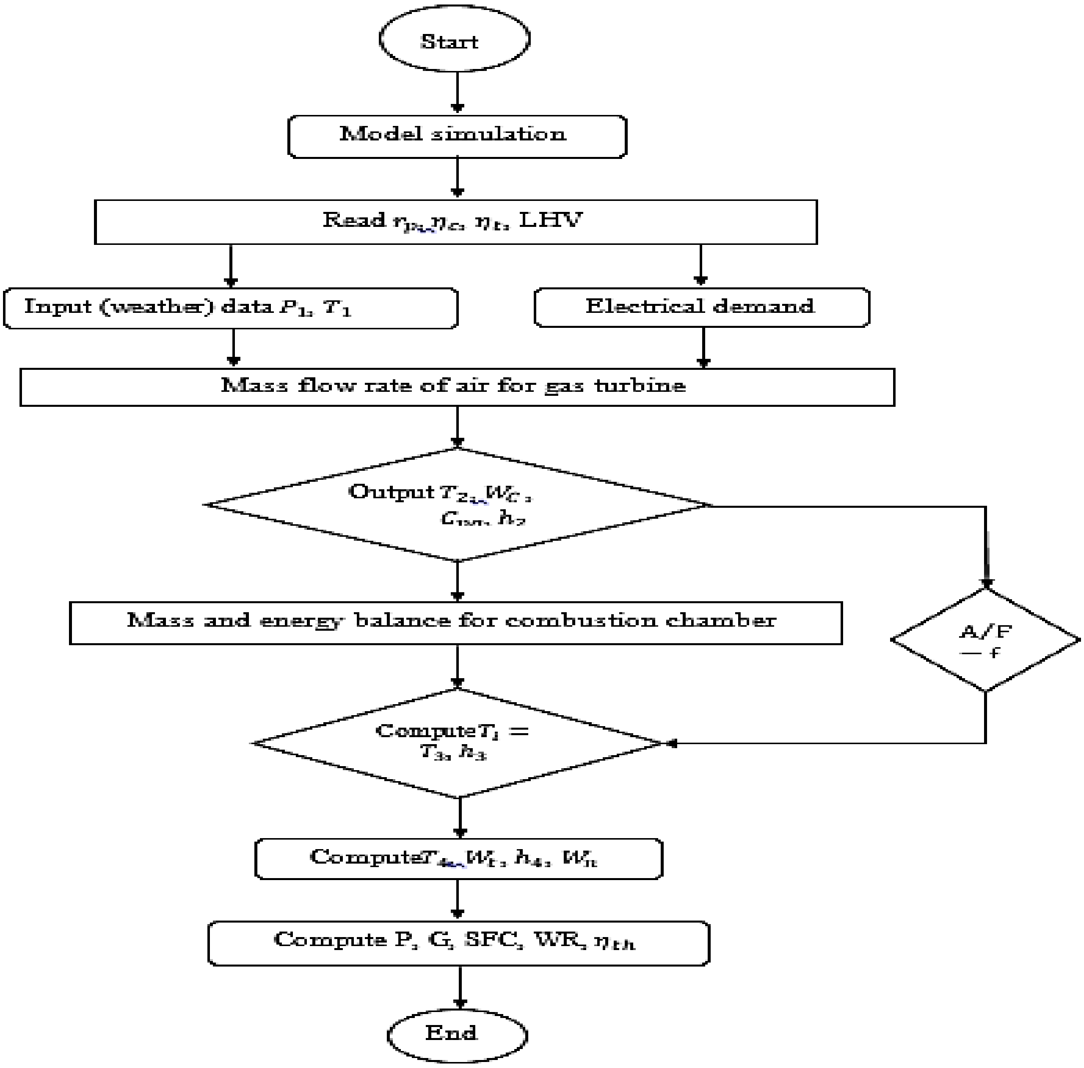

Fig. 3 – Flowchart Simulation of the Performance Process of a Gas Turbine Power Plant

3. Results and Discussion

This section presents the simulation findings about the impact of operating conditions on the efficiency of gas turbine power plants. The performance of gas turbine plants is studied in relation to operating conditions like AT and RH. The effects of operating conditions on power output, compressor power consumption, work ratio (WR), SFC, heat supply, exhaust energy, and efficiency are calculated using an energy-balanced computational model and ODE45 algorithm found in MATLAB R2007b software. Fig. 3 depicts a flowchart of the simulation of the performance process for a gas turbine power plant. To show how sensitive gas turbine performance is to environmental factors, this study specifically considers operational atmospheric conditions. In this study, the basic parameters used are those of the Transcorp power plant (Delta IV) in Ughelli, Delta State, Nigeria, and the simulation assumes ideal conditions for the turbine and compressor work transfer processes.

3.1 The Influence of AT

Fig. 4 shows how AT and RH affect compressor power. This specifically refers to the amount of effort required to operate the air compressor in relation to the AT and RH. Fig. 4 demonstrates that as AT increases at constant RH, the compressor's power consumption rises and that as RH rises at constant AT, the compression power soars.

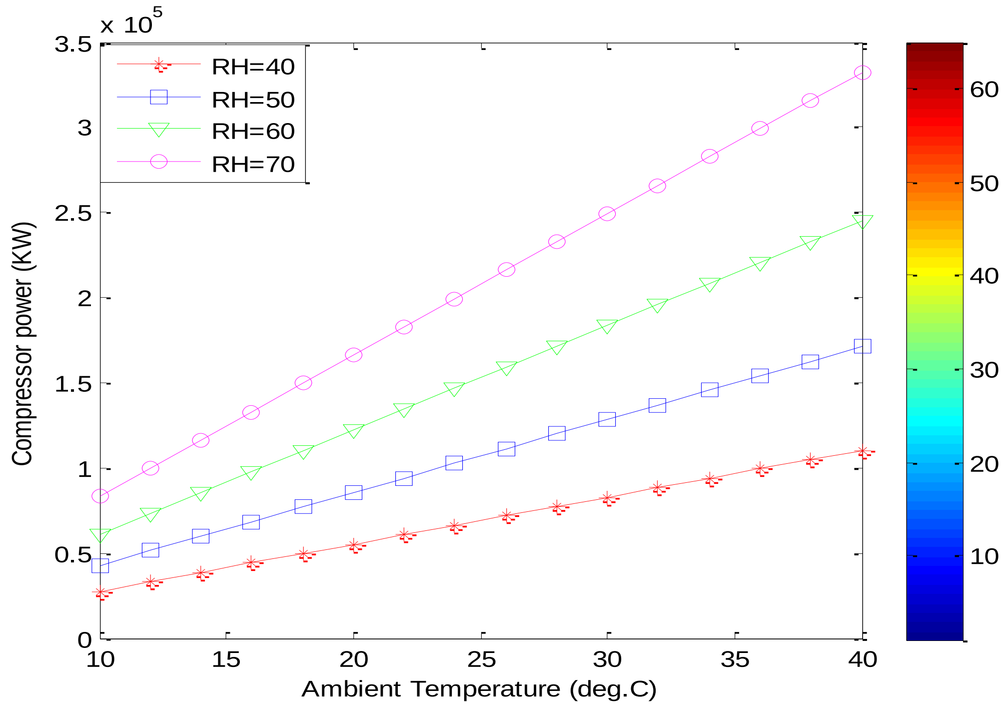

Fig. 4 – The influence of AT and RH on compressor power

This increase is due to the high moisture content in the air stream at high RH, as well as the fact that it takes more power to compress a gas at a high temperature than at a low temperature for the same pressure ratio. At a temperature of 20 ºC., for example, a 25% increase in RH results in a 55% increase in compression power. The result shows that the compressor turbine works best in conditions with low RH and AT. As a result, the best performance is obtained at relatively low AT and RH. Fig. 4 demonstrates that more power is used when the RH rises from 40 to 70%.

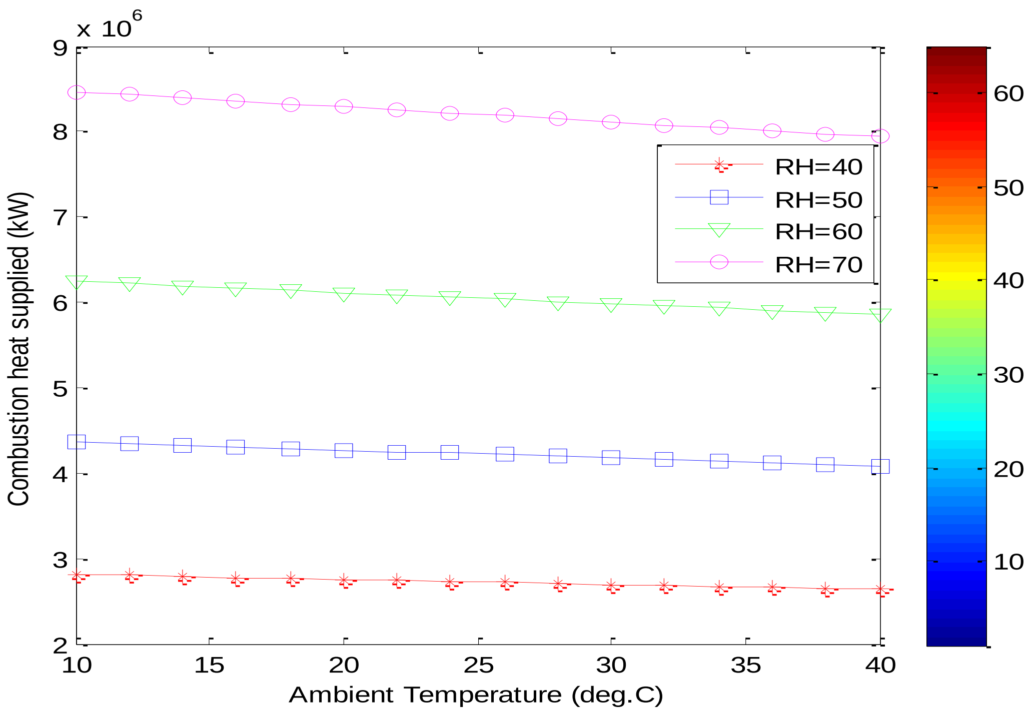

Fig. 5 – Impact of AT and RH on combustion heat supplied

Fig. 5 depicts the required heat supply to power the gas turbine power plant as a function of AT and RH. Fig. 5 shows that the heat supply requirement decreases slightly as the AT increases at constant RH, but significantly increases as the RH increases due to the high moisture content per kg of dry air. As a result, the combustion process prefers low RH and AT. Similarly, at 20 ºC AT, a 25% increase in RH results in a 55% increase in heat supply requirement. As the RH increases from 40 to 70%, more combustion heat is supplied. As a result, the plant's operating costs increase with an increase in RH in terms of fuel cost.

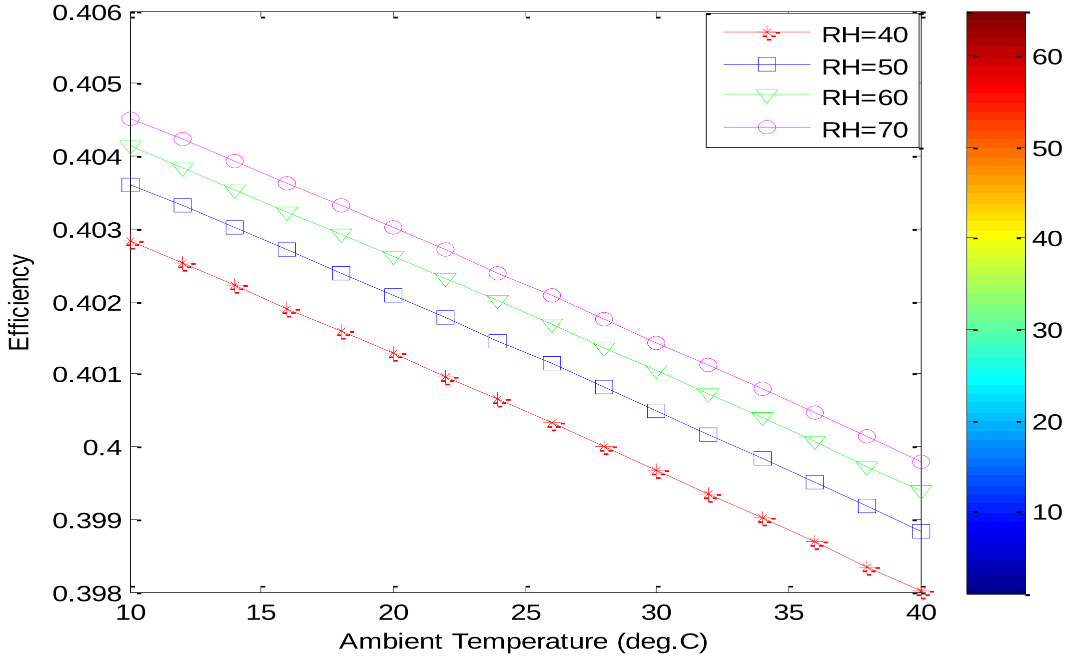

Fig. 6 – Impact of AT and RH on plant efficiency

The impact of AT and RH on plant efficiency is depicted in Fig. 6. Fig. 6 depicts how plant efficiency decreases rapidly as AT increases at constant RH and increases as RH increases. This increase in efficiency as a result of lower RH and AT is due to lower compressor power consumption at lower RH and AT, as well as a reduction in heat quality supplied. Okafor [32] reported a similar result when considering only AT. A change in RH from 40 to 50% results in a 0.022% increase in cycle efficiency at an AT of 20 ºC. This cycle efficiency is highest when RH and AT are low. Fig. 6 clearly shows that the efficiency decreases as the RH rises from 40% to 70%. A lower AT results in a lower RH and less compressor work, which results in a greater gas turbine output power. Fig. 6 illustrates how changes in RH and compressor work affect the efficiency of gas turbine plants.

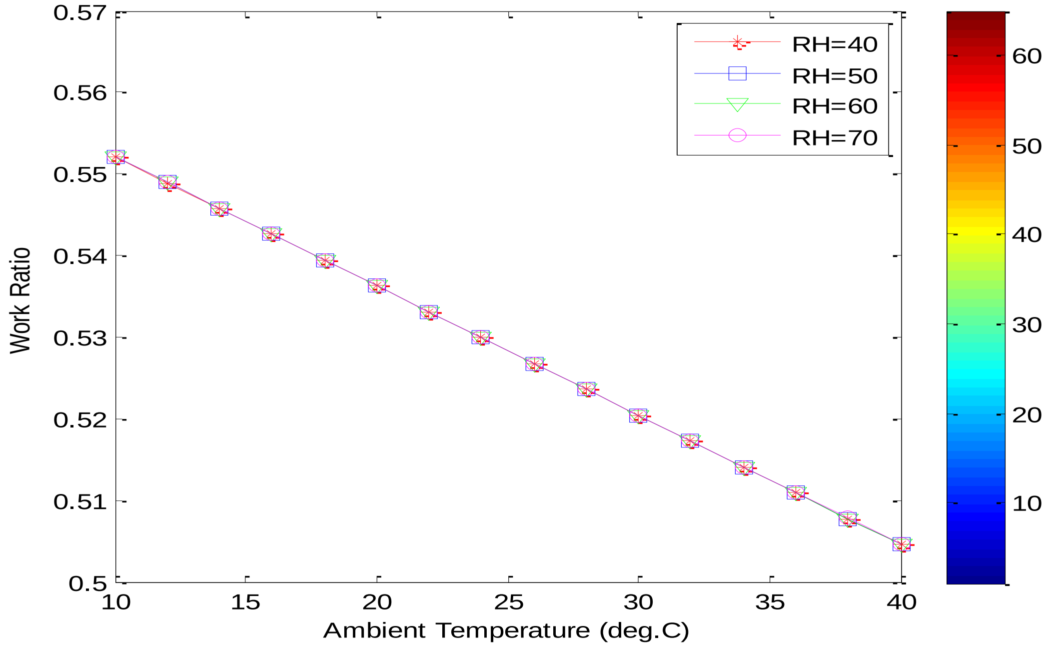

Fig. 7 – Impact of RH and AT on plant WR

Fig. 7 shows how AT and RH affect the plant WR. The WR decreases significantly as the AT increases and is relatively unaffected by RH, as evidenced by the overlap of the curves at various RH levels, as shown in Fig. 7. The WR rises in direct proportion to the ratio of turbine inlet temperature to compressor inlet temperature because a significant portion of the power delivered by the turbine is used to drive the compressor and because the engine network depends on the excess of turbine work over compressor work. Ibrahim and Rahman [28] used AT and compressor ratio as parameters and found a similar trend.

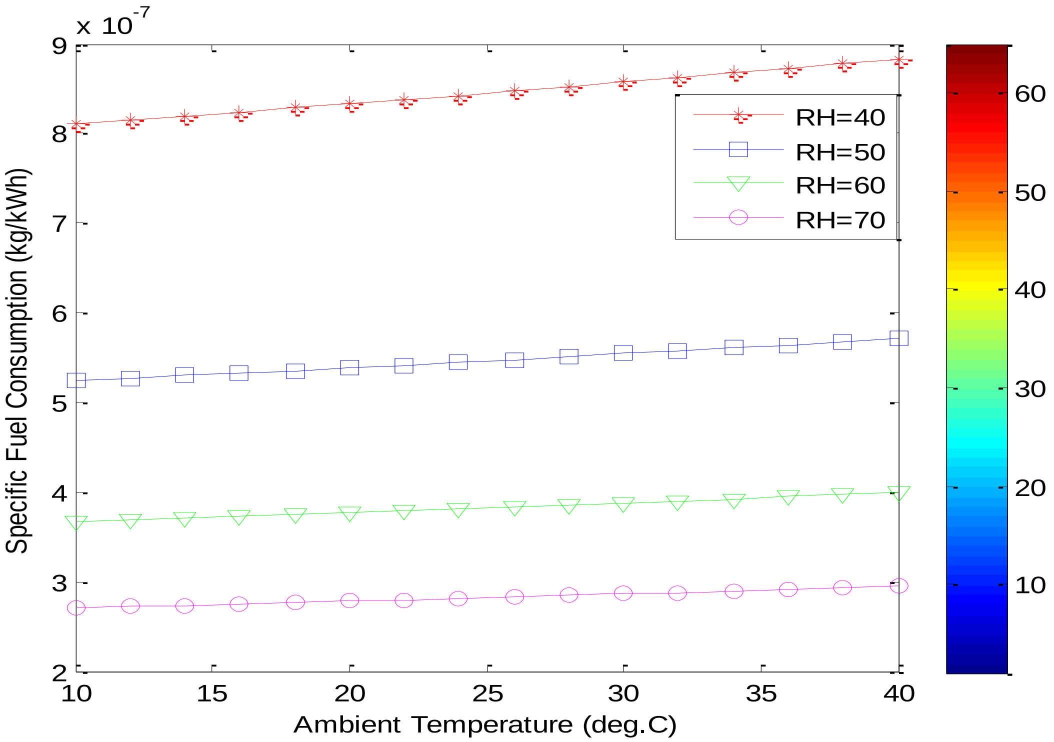

Fig. 8 – The influence of AT and RH on SFC

The relationship between SFC, RH and AT is depicted in Fig. 8. At low AT, the SFC increases slightly with increasing AT and RH. The effect of variation in SFC is more pronounced at higher AT and RH. The SFC decreases from 0.9 to 0.25 kg/kWh as the RH rises from 40% to 70% and the AT rises from 10 to 40 ºC. This behavior is caused by the fact that at low RH, the mass flow through the turbine is reduced due to low moisture content in the air stream, requiring more fuel for augmentation if the turbine is to deliver its rated power. At a temperature of 20 ºC, a drop in RH of 20 to 60% results in a 35% increase in SFC.

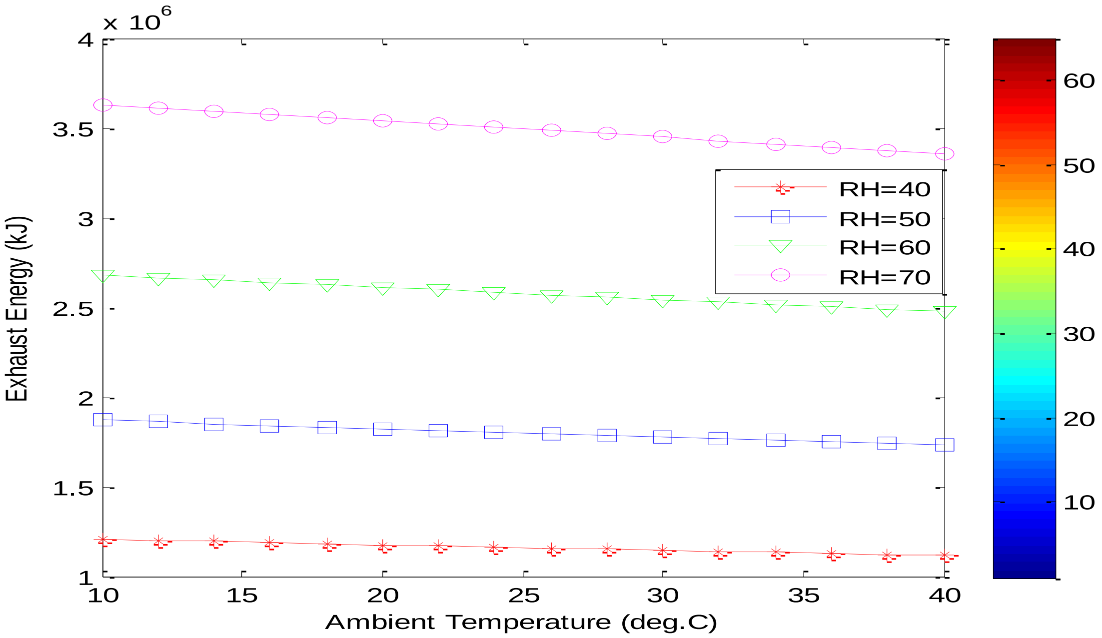

Fig. 9 – The impact of RH and AT on exhaust energy

The variation of the energy carried away by the flue as a function of AT with varying RH is depicted in Fig. 9. Fig. 9 clearly shows that the exhaust energy decreases with increasing AT at constant RH and increases astronautically with increasing RH. When the intake air temperature is reduced, the flow rate of the exhaust gas increases proportionally. The high moisture content and high enthalpy of the vapour in the exhaust stream cause an increase in exhaust energy and a corresponding increase in RH. At a temperature of 20 °C, a change in RH from 40% to 50% results in a 55% increase in exhaust energy.

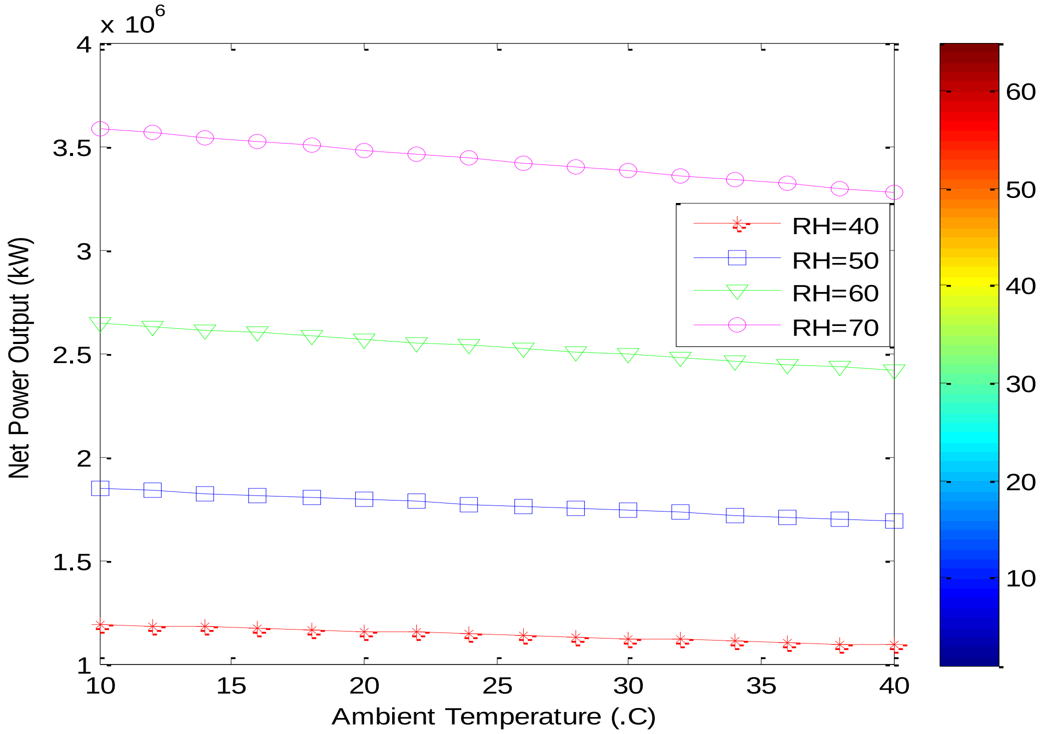

Fig. 10 – The influence of RH and AT on net power output

Fig. 10 depicts a plot of net power output against RH and AT. Fig. 10 demonstrates that the net power output reduces marginally when the RH increases at a constant temperature, but significantly increases as the RH increases at a constant temperature. This is explained as follows: first, at lower AT, the compressor power consumption decreases; second, at high RH, the moisture content is quite high, causing a larger mass flow rate to expand in the turbine, increasing net power output. Basha et al. [33] and González-Díaz et al. [34] found a similar trend considering only AT.

4. Conclusion

The following conclusion was reached using a thermodynamic model to analyze and evaluate the performance of a gas turbine power plant by considering the AT, RH, and other conditions of the inlet air;

1. The gas turbine underwent a thorough analysis of environmental factors such as AT and RH due to the importance of efficient operation and low emissions for the environment.
2. The simulation results from parameter modeling revealed that AT and RH have an impact on the performance of a gas turbine power plant.
3. The results clearly showed that for every 0.7% increase in AT, compressor power consumption increased by 2.5%, and for every 25% increase in RH, compressor power requirement and heat supply increased by 55%.
4. The efficiency analysis reveals that as RH increases from 40% to 50%, cycle efficiency decreases by 0.022%. Net power output, on the other hand, increases as RH increases.
5. The peak overall thermal efficiency occurs when the ambient temperature is high.
6. SFC increased as AT increased; SFC increased by 0.25% for every 2.25% increase in AT.
7. In response to a 1.85 % increase in AT, net power and net power output decreased by 0.23 and 0.68 %, respectively.
8. The exhaust energy decreases with increasing AT and RH. When the intake air temperature is reduced, the flow rate of the exhaust gas increases proportionally. At a temperature of 20 °C, a change in RH from 40% to 50% results in a 55% increase in exhaust energy.
9. The impact of changes in AT on net power output, total power, WR, and thermal efficiency is greater than the effect of changes in RH ratio.

As a result, it is concluded that both ambient temperature and relative humidity have a significant impact on the operation of the gas turbine power plant. Further research should focus on fuel cell integration, sustainability, and gas turbine performance sensitivity analysis.

References

[1] Akroot A, Saif E. Comparative energy analysis on a combined power plant of gas turbine and stirling engine. *Int. J. Adv. Res. Eng. Technol. & Sci.*. 2019; 6(4): 1-9.

[2] Direk M, Mert MS. Comparative and Exergetic study of a Gas turbine system with Inlet air cooling. *Technical Gazette*. 2018; 25, Suppl. 2: 306-311.

[3] Mehaboob B., Shaahid SM., AL-Hadrami L. Impact of fuels on performance and effiency of Gas Turbine Power Plants. *Energy Procedia*. 2012; 14: 558-565.

[4] Fernandez DAP, Foliaco B, Padilla RV, Bula A, Gonzalez-Quiroga A. High ambient temperature effects on the performance of a gas turbine-based cogeneration system with supplementary fire in a tropical climate. *Case Studies in Thermal Engineering*. 2021; 26: 101206.

[5] Allakulyyev Sh, Altyyev B, Saryyev M, Hojalyyev A, Danatarova M. Scientific-technical analysis of the ambient temperature effect on the power of gas turbine installation in the conditions of Turkmenistan. *IOP Conf. Series: Earth and Environ Sci.* 2022; 1045: 012164.

[6] Ukwamba SI, Orhorhoro EK, Omonoji AA. Performance Evaluation of A simple gas turbine power plant using vapour Absorption chiller. *IOSR Journal of Mechanical and Civil Engineering*. 2018; 15 (2): 13-18.

[7] Abdulrahim AH, Chung JN. Performance improvement of cogeneration plants in hot arid region via sustainable turbine inlet air cooling technologies: An energy-water nexus comparatives case study. *Int. J. Energy Research*. 2021; 45(7): 10765 – 10793.

[8] Chukwuneke JL, Achebe CH, Nwosu MC, Sinebe JE. Analysis and Simulation on Effect of Head and Bucket Splitter Angle on the Power Output of a Pelton Turbine. *International Journal of Engineering and Applied Sciences*. 2014a; 5(3): 1 – 8.

[9] Sinha AA, Choudhary T, Ansari MZ, Sanjay ME. Estimation of exergy-based sustainability index and performance evaluation of a novel intercooled hybrid gas turbine system. *Int. J. Hydrogen Energy*. 2023a; 48(23): 8629 – 8644.

[10] Chukwuneke JL, Okechi LE, Unegbu CI, Ekechi AT, Madumere AU, Okeke JC, & Odeh CP. Impact of parameters on gas turbine performance using energy analysis. *Journal of Energy Research and Reviews*. 2025; *17*(4), 53–64.

[11] Saif M, Tariq M. Performance Analysis of gas turbine at varying ambient temperature. *Int. J. Mech. Eng. & Technol.* 2017; 8(1): 270-280.

[12] Chukwuneke JL, Achebe CH, Okolie PC, Okwudibe HA. Experimental Investigation on Effect of Head and Bucket Splitter Angle on the Power Output of a Pelton Turbine. *International Journal of Energy Engineering*. 2014b; 4(4): 81 – 87.

[13] Sinha AA, Saini G, Sanjay ME, Shukla AK, Ansari MZ, Dwivedi G, Choudhary T. A novel comparison of energy-exergy, and sustainability analysis for biomass-fueled solid oxide fuel cell integrated gas turbine hybrid configuration. *Energy Conversion and Management*. 2023b; 283: 116923.

[14] Choudhary T, Sahu MK, Sanjay R, Kumari A, Mohapatra A. Thermodynamic modeling of blade cooled turboprop engine integrated to solid oxide fuel cell: a concept. *SAE Technical Paper*. 2018; doi.org/10.4271/2018-01-1308.

[15] Igoma EN, Amadnobogha C, Osia IO. Parametric appraisal of the performance of a gas turbine ultilizing comparative breakdown of the performance criteria. *Int. Research J. Modernization in Eng. Technol.* 2022; 4(4): 649 – 657.

[16] Gollamudi S, Kommineni R, Valdlamudi TC, Katuru BP. Investigation of regenerative gas turbine performance under the influence of dynamic atmospheric conditions in India using energy and exergy analysis. *Int. J. Heat and Technol.* 2023; 41(2): 309 - 375

[17] Al-Tobi I. Performance Enhancement of Gas Turbines by Inlet Air cooling. *International Conference on Communication, Computer and Power (ICCCP[1]09). Muscat.* 2009 Februrary; 15-18: 165-170.

[18] Mahapatra AK, Sanjay BE. Performance Analysis of an air humidifier integrated gas turbine with film air cooling of turbine blade. *Journal of Energy in Southern Africa*. 2013; 24(4):71-81.

[19] Choudhary T, Sanyoy ME. Thermodynamic assessment of advanced SOFC-blade cooled gas turbine hybrid cycle. *Int. J. Hydrogen Energy*. 2017; 42(15): 10248 – 10263.

[20] Arabi SM, Ghadamian H, Aminy M, Ozgoli HA, Ahmadi B, Khodsiani M. The energy analysis of F_5 gas turbines inlet air-cooling systems by the off-design method. *Measurement and Control*. 2019: 1-10.

[21] Shireef LT, Ibrahim TK. Influence of operating parameters on the performance of combined cycle based on exergy analysis. *Case studies in Thermal Engineering*. 2022; 40: 102506.

[22] Anand B, Murugavelh S. Performance analysis of a novel augmented desalination and cooling system using modified vapor compression refrigeration integrated with humidification-dehumidification desalination. *J. Cleaner Prod.* 2020; 255: 120224.

[23] Edafiadhe ED, NwobiOkoye CC, Madu KE, Chukwuneke JL. Predictive modelling for parametric analysis of an air conditioning system in a 400-seat auditorium in Warri, sub-tropical Nigeria. *Journal of Engineering Research and Reports*. 2022; 23(5): 59 – 67.

[24] Lui W, Zhang X, Zhao N, Shu C, Zhang S, Ma Z, Han J. Performance analysis of organic Ranknie Cycle power generation system for inter cooled cycle gas turbine. *Advances in mechanical Engineering*. 2018; 10(8): 1-12.

[25] Oyedepo SO, Fagbenle RO, Adefila SS. Modelling and Assessment of effect of operation Parameters on Gas Turbine Power Plant Performance using First and Second Laws of Thermodynamics. *American Journal of Engineering and Applied Sciences*. 2016; 10(2): 412 – 430.

[26] Ujam JA, Chukwuneke JL, Achebe CH, Ikwu GOR. Modeling the Effect of Head and Bucket Splitter Angle on the Power Output of a Pelton Turbine. *International Journal of Engineering and Applied Sciences*. 2014; 5(3): 26 – 36.

[27] Mishra RS, Agarwal S. Performance Parametric analysis of retrofitted gas turbine Cycle using STIG and Evaporative cooling techniques. *Int. J. Res. Eng. &Inno.*, 2018; 2(5) : 469-483.

[28] Ibrahim TK, Rahman MM. Effect of compression Ratio on performance of combined cycle Gas Turbine. *Int. J. Energy Eng.* 2012; 2(1):9-14.
[29] Ana PPS., Clandia RA, Edson LZ. Comparison of different Gas Turbine Inlet Air Cooling Methods. *World Academy of Science, Engineering and Technology*. 2012; 6(1), 1–6.
[30] Ibrahim TK, Mohammed MK, Al-Doori WHA, Al-sammarraie AT, Basrawi F. Study of the performance of the gas turbine power plants from the simple to complex cycle: A Technical review. *Journal of Advanced Research in fluid mechanics and Thermal Sciences*. 2019; 57(2): 228-250.
[31] Naradasu RK, Konijeti RK, Alluru VR. Thermodynamic analysis of heat recovery steam generator in combined cycle power plant. *Therm. Sci.*. 2007; 11(4): 143-156.
[32] Okafor V. Thermodynamic analysis of compressor inlet air precooling techniques of a gas turbine plant operational in Nigeria energy utility sector. *International Journal of Engineering Science Technologies*. 2020; *4*(2), 13–24.
[33] Basha M, Shaahid SM, Al-Hadhrami L. Impact of fuels on performance and efficiency of gas turbine power plants. *Energy Procedia*. 2012; *14*, 558–565.
[34] González-Díaz A, Alcaráz-Calderón AM, González-Díaz MO, Méndez-Aranda Á, Lucquiaud M, González-Santaló JM. Effect of the ambient conditions on gas turbine combined cycle power plants with post-combustion CO2 capture. *Energy*. 2017; *134*.